Observation of π Stark Components in Microwave Spectroscopy: Precision Measurements on HCN*

BROJO N. BHATTACHARYA† AND WALTER GORDY
Department of Physics, Duke University, Durham, North Carolina
(Received February 4, 1960)

A parallel plate Stark cell has been designed and constructed for the millimeter wave region of the spectrum. With the cell both π and σ Stark components can be observed. High precision Stark effect measurements have been made on the π and σ components of the $J=0\rightarrow 1$ transition of HCN^{14}. From these the electric dipole moment of HCN in the ground vibrational state has been calculated to be 2.985 ± 0.005 Debye units.

INTRODUCTION

MOST of the earlier methods for deducing dipole moments consisted of extrapolating this molecular property from bulk properties. However, with microwave spectroscopic techniques it is now possible to evaluate dipole moments more directly by measurement of the Stark effect on rotational lines.

Once the dipole moment of a molecule is known accurately it can serve as a standard for comparative measurements. Because HCN has very strong lines in the 3-mm region it could presumably serve as such a standard. Although N^{14} has a quadrupole moment, this is not considered a serious difficulty since the strong field case is very readily reached and since there is one line in the $\Delta M=\pm1$ transitions which is not degenerate.

The present report includes results of Stark measurements for the π as well as σ components of HCN. So far as we are aware, these measurements are the first to be made of π Stark components in the microwave rotational spectrum of any molecule. Earlier, less accurate measurements[1] have been made of the σ Stark components of the $J=0\rightarrow 1$ rotational transition of HCN, and an earlier value of the dipole moment for an excited vibrational state has been deduced from the Stark splitting of l-doublet transitions.[2]

EXPERIMENTAL ASPECTS

The absorption cell conventionally used for observations of the Stark effect in microwave spectroscopy is that described by McAfee, Hughes, and Wilson.[3] It consists of a rectangular waveguide operated in a TE_{0n} mode with a planar central electrode perpendicular to the E plane, held and insulated from the waveguide by means of plastic strips along the sides of the guide. With this arrangement, the static field is always parallel to the E vectors of the microwave field. Hence, only, $\Delta M=0$, transitions can be observed. Also, insulation problems make difficult the application of a high field between the electrodes.

To avoid these difficulties and to make possible observations of the σ, or $\Delta M=\pm1$, transitions, we decided to construct a parallel plate cell. Such a microwave Stark cell was proposed by one of us[4] and has been previously used in this laboratory.[5,6] A similar cell has been constructed and used in the high-precision measurements of the dipole moment of OCS by Marshall and Weber,[7] at the National Bureau of Standards. The present work, however, represents the first adaptation of the cell to the measurement of π Stark components, and to high-precision measurements in the shorter millimeter wave region.

In order to feed microwave power to the parallel plate cell, horns were used as matching devices. For observation of the σ components, the horns were made so that the E plane tapers to the shorter cross section of the cell and the H plane tapers to the longer section. Under such conditions the E vector of the radiation field is perpendicular to the plane of the parallel plates and hence is parallel to the dc Stark field. The mode propagated for this arrangement, the TEM mode, has no limiting cut-off frequency. The wavelength in the cell and the effective cell length are the same as the free space values. For observation of the π components, the horns were made so that the E plane tapers to the longer cross section of the cell. Except for distortions at the edges of the plates, the E vector of the radiation field is then parallel to the cell plates and perpendicular to the static electric field. The dominant mode propagated for this arrangement is the TE_1 mode, which has a cut-off wavelength of $\lambda_c=2d$, where d is the distance between the plates. The wavelength in the cell is $\lambda_g=\lambda/[1-(\lambda/\lambda_c)^2]^{\frac{1}{2}}$, and the effective cell length is $\lambda_{eff}=l(\lambda/\lambda_c)$, where l and λ are the corresponding free space values.

The horns were made of copper electroformed around Lucite forms machined to the proper dimensions and coated with a conducting paint. The different modes

* This research was supported by the U. S. Air Force through the Air Force Office of Scientific Research of the Air Research and Development Command.
† Present address: Indian Institute of Technology, Bombay, India.
[1] S. N. Ghosh, R. Trambarulo, and W. Gordy, J. Chem. Phys. **21**, 308 (1953).
[2] R. G. Schulman and C. H. Townes, Phys. Rev. **77**, 421 (1950).
[3] K. B. McAfee, Jr., R. H. Hughes, and E. B. Wilson, Rev. Sci. Instr. **20**, 821 (1949).
[4] W. Gordy, Revs. Modern Phys. **20**, 668 (1948).
[5] R. F. Trambarulo and C. F. Luck, Phys. Rev. **87**, 172 (1952).
[6] O. Fujii, M. A. thesis, Duke University, 1954 (unpublished).
[7] S. A. Marshall and J. Weber, Rev. Sci. Instr. **28**, 134 (1957).

excited in this manner were exceedingly pure, and one of the patterns, either σ or π depending on the horns being used, was completely absent when the other was observed. It was also found that the cell attenuation for the *TE* mode excited by the second kind of horns was not noticeably greater than that for the *TEM* mode.

The first cell employed was made of two $\frac{1}{4}$-in. thick aluminum plates, approximately 51 cm×7.5 cm. One side of the plates was accurately machined and polished with rouge to give a mirror-like finish. In a later model the cell plates were made of Pyrex, ground, polished, and silver-plated. Quartz spacers, accurately ground for uniform thickness were evenly placed near the edges along the length of the cell, four on each side. Aluminum strips, slightly wider than the plate itself, were screwed on the outer sides of the plate, and these were lightly screwed on Teflon posts so as to give mechanical strength and rigidity while the separation was maintained by the glass separators.

The finished cell was enclosed in a glass pipe with outlets for electrodes and vacuum system, the ends being sealed with glass plates glued to the pipe by means of cold-setting epoxy resins. The Pyrex plates had openings of dimensions slightly larger than the cross section of the cell, which were sealed off with mica of thickness barely adequate to withstand the strain of evacuation.

To produce the Stark splitting, a static electric field was applied across the cell plates. The source of the static field was a bank Burgess *XX* 45 batteries joined in series. Measurement of the voltage was made by use of an accurately calibrated voltage divider and a type *K* potentiometer (Leeds and Northrup). With dry cells the voltage fluctuates because of polarization, but this fluctuation can be avoided through use of a high-resistance voltage divider. The voltage was averaged over that before and after each observation. Multiple observations, five or higher in case of doubt, were taken around the same potential.

A video-sweep detecting system with a broad-banded, high fidelity video amplifier was employed for the measurements. The millimeter wave power was generated and detected with devices already described.[8] Frequency measurements were made with a frequency multiplier chain[9] monitored by Station WWV.

THEORY

The theory of the Stark effect on the rotational spectra of linear molecules with hyperfine structure has been developed by Fano.[10] The terms of the Hamiltonian relevant to the present investigation are:

$$H=H_R+H_E+H_q+H_C$$
$$=\mathbf{P}^2/2B-\boldsymbol{\mu}\cdot\mathbf{E}+P(J,I)[3(\mathbf{I}\cdot\mathbf{J})^2+\tfrac{3}{2}(\mathbf{I}\cdot\mathbf{J})+I^2J^2]+C(\mathbf{I}\cdot\mathbf{J}),$$

where $P(J,I)=-eQq/4I(2I-1)(2J-1)(2J+3)$. Here H_R is the Hamiltonian corresponding to the rotational energy, H_E is the Stark interaction, H_q is the nuclear quadrupole interaction, and H_C is the nuclear magnetic interaction with the molecular rotational magnetic field. The nature of the solution for the energy eigenvalues depends upon the relative values of the terms in H. Here we shall give the solutions which apply specifically to HCN.

In HCN the nuclear interactions H_q and H_C are small, and the strong-field, Back-Goudsmit case is easily achieved except for the $M_J=\pm1$ levels. There are nondiagonal elements connecting $M_J=\pm1$ and $M_I=\pm1$ which cause a breakdown of the $M_J=\pm1$ degeneracy. Except for $J=0$ or $M_J=\pm1$ the strong field formula,[11]

$$W_{JIM_JM_I}=W_{JM_J}^{(2)}-\frac{eQq}{4}\frac{3M^2-I(I+1)}{I(2I-1)}\times\frac{3M_J^2-J(J+1)}{(2J-1)(2J+3)}+CM_JM_I,$$

applies, where $W_{JM_J}^{(2)}$ represents the Stark effect energy of a linear molecule without hyperfine structure and is

$$W_{JM_J}^{(2)}=-\frac{\mu^2E^2}{2Bh}\frac{3M_J^2-J(J+1)}{J(J+1)(2J-1)(2J+3)}.$$

For the $J=0$ the nuclear interactions make no contributions, and

$$W_{0I0M_I}^{(2)}=-\mu^2E^2/6Bh.$$

In the present study we need also the energy eigenvalues for the special $M_J=\pm1$ case for which the strong field formulas do not apply. To obtain them we must solve the secular equation

$$\begin{vmatrix} W_{J,I,1,-1}^{(2)}+\langle J,I,1,-1|H_q+H_C|J,I,1,-1\rangle-W & \langle J,I,1,-1|H_q+H_C|J,I,-1,1\rangle \\ \langle J,I,-1,1|H_q+H_C|J,I,1,-1\rangle & W_{J,I,-1,1}^{(2)}+\langle J,I,-1,1|H_q+H_C|J,I,-1,1\rangle-W \end{vmatrix}=0.$$

[8] W. C. King and W. Gordy, Phys. Rev. **93**, 407 (1954).
[9] W. Gordy, W. V. Smith, and R. F. Trambarulo, *Microwave Spectroscopy* (John Wiley & Sons, Inc., New York, 1953), Chap. I.
[10] U. Fano, J. Research. Natl. Bur. Standards **40**, 215 (1948).
[11] Reference 9, Chap. III.

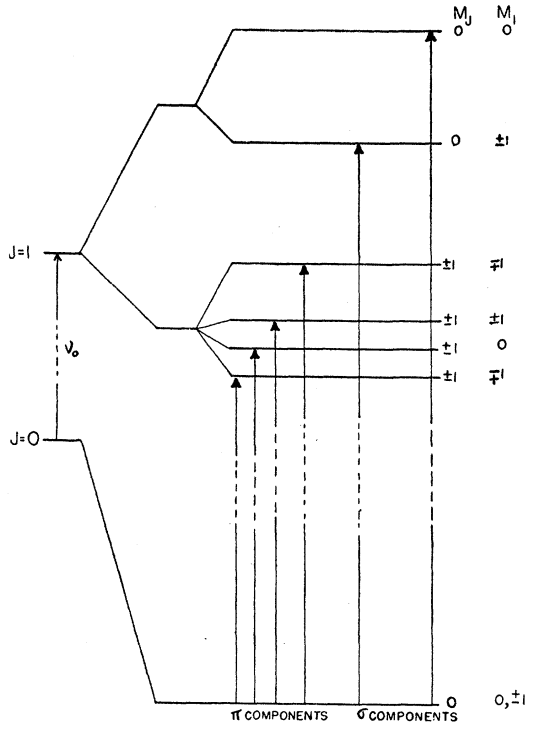

FIG. 1. Energy level diagram (not to scale) indicating the π and σ Stark components of the $J=1\leftarrow 0$ transition of HCN.

By substitution of the appropriate matrix elements[12] and by solving this equation we obtain the following formulas for the $M_J=\pm 1$ levels.

$$W=W_{J,|M_J|=1,I,M_I}$$

$$=W^{(2)}_{J,|M_J|=1}+\frac{eQq}{4I(2I-1)}R(J,1)\times[3(M^2+1)-I(I+1)]-C$$

$$\pm\left\{\left[CM-\frac{3}{2}\frac{eQq}{4I(2I-1)}R(J,1)M\right]^2+\frac{3}{2}\left[\frac{eQq}{4I(2I-1)}S(J)\right]^2(I^2-M^2)\times[(I+1)^2-M^2]\right\}^{\frac{1}{2}},$$

where

$$R(J,M_J)=[J(J+1)-3M_J^2]/(2J-1)(2J+3)$$

and

$$S(J)=-(\tfrac{3}{2})^{\frac{1}{2}}J(J+1)/(2J-1)(2J+3).$$

With the aid of the formulas given above, it is possible to write the following equations for the different fine structure components of the $J=0\rightarrow 1$ transition observed in the strong field limit. For $\Delta M_J=\pm 1$ (π components):

$$M_J=\pm 1,\quad M_I=\mp 1\leftarrow M_J=0,\quad M_I=\pm 1$$
$$\Delta\nu=(7/30)(\mu^2E^2/2B_0h)+0.25eQq-C,$$
$$M_J=\pm 1,\quad M_I=0\leftarrow M_J=0,\quad M_I=0$$
$$\Delta\nu=(7/30)(\mu^2E^2/2B_0h)+0.1eQq-C,$$
$$M_J=\pm 1,\quad M_I=\pm 1\leftarrow M_J=0,\quad M_I=\pm 1$$
$$\Delta\nu=(7/30)(\mu^2E^2/2B_0h)-0.05eQq+C,$$
$$M_J=\pm 1,\quad M_I=\mp 1\leftarrow M_J=0,\quad M_I=\pm 1$$
$$\Delta\nu=(7/30)(\mu^2E^2/2B_0h)-0.35eQq-C.$$

For $\Delta M=0$ (σ components):

$$M_J=0,\quad M_I=\pm 1\leftarrow M_J=0,\quad M_I=\pm 1$$
$$\Delta\nu=(8/15)(\mu^2E^2/2B_0h)+0.1eQq,$$

and

$$M_J=0,\quad M_I=0\leftarrow M_J=0,\quad M_I=0$$
$$\Delta\nu=(8/15)(\mu^2E^2/2B_0h)-0.2eQq.$$

Figure 1 gives a general strong field disposition of the levels for $J=0$, 1 and $I=1$. The different interactions are not drawn to scale. The transitions shown give a general idea of the splitting for π and σ components. In these expressions $\Delta\nu$ represents frequency displacements, μ is the molecular dipole moment, E is the applied field strength, $B_0=h/8\pi^2I$ when I is the moment of inertia of the molecule, eQq is the nuclear quadrupole coupling, and C is the nuclear magnetic coupling constant.

RESULTS

The molecular constants of HCN will be used extensively throughout the calculations. It was therefore thought necessary to remeasure the frequency of the $J=1\leftarrow 0$ transitions accurately. An extensive set of measurements, with the 10 Mc/sec frequency broadcast by Station WWV employed as a standard, was accordingly made. The averaged values obtained for the frequencies of the HCN lines together with the molecular constants calculated from them are given in Table I. Also listed in Table I is the final value which we

TABLE I. Measured rotational frequencies and molecular constants for $HC^{12}N^{14}$.

Transition $J=1\leftarrow 0$	Frequency in Mc/sec
$F=1\leftarrow 1$	88 630.431±0.005
$2\leftarrow 1$	88 631.871±0.005
$0\leftarrow 1$	88 633.954±0.005
Molecular constants	
$\nu_0=88\,631.623$ Mc/sec	
$eQq=-4.714$ Mc/sec	
$C=0.013$ Mc/sec	
$\mu=2.985\pm0.004$ Debye units	

[12] N. F. Ramsey, *Nuclear Moments* (John Wiley & Sons, Inc., New York, 1953).

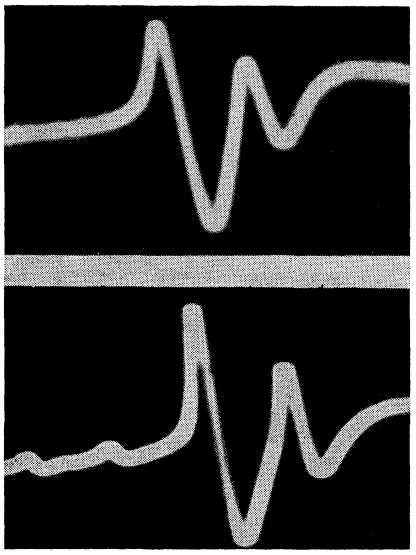

FIG. 2. Cathode ray oscillograms of the σ components for the intermediate (lower) and strong (upper) field splitting of the $J=1 \leftarrow 0$ transition of HCN.

obtain for the electric dipole moment of the molecule in the ground vibrational state.

The general splitting patterns of the $\Delta M=0$ transitions, intermediate and high field, are shown in the oscillograms reproduced in Fig. 2. In all the oscillograms reproduced, the frequency increases from left to right. No distinction is made between the weak and intermediate field case because the quadrupole interaction is so small that the interaction caused by nondiagonal terms must be taken into account at even the lowest fields employed.

The dependence of the frequency shifts of the σ components on E^2 is indicated by the solid lines in Fig. 3. As the potential across the Stark cell is raised, the low-frequency lines disappear around 800 volts/cm, and one gets the strong field pattern consisting of two strong lines corresponding to

$$M_J=0, \quad M_I=\pm 1 \leftarrow M_J=0, \quad M_I=\pm 1$$

and

$$M_J=0, \quad M_I=0 \leftarrow M_J=0, \quad M_I=0,$$

in order of increasing frequency, as is expected from the energy level diagram in Fig. 1.

The lines in the $\Delta M=\pm 1$ or π transitions are rather numerous in the low or intermediate field case, and they could not be properly resolved. Thus it was possible to study the π transitions only in the strong field case. An oscillogram showing the π components for a strong field is given in Fig. 4. The strong field pattern consists of four lines, as would be expected from the energy level diagrams of Fig. 1. The variation in frequency of the π components with field in the strong field region is indicated by the dotted lines of Fig. 3.

The frequency shifts of one of the σ lines from the origin of the $J=1 \leftarrow 0$ line (the ν_0 frequency of Table I) of HCN are given in Table II. The field, in volts/cm, is the root mean square of the field of several observations. Since it was difficult to keep the voltage absolutely constant because the frequency shifts depend primarily on E^2, it was thought that the root mean square voltage would be more representative. The dipole moment has been calculated only for the $M_J=0, M_I=\pm 1 \leftarrow M_J=0, M_I=\pm 1$ components because the other lines are roots of cubic equation or because the frequency shifts are too small for accuracy. The results of the dipole moment calculations are also given in Table II. The formula used for calculation of the dipole moment for the above mentioned line is the one for the intermediate field case, obtained by solution of the secular equation, for the

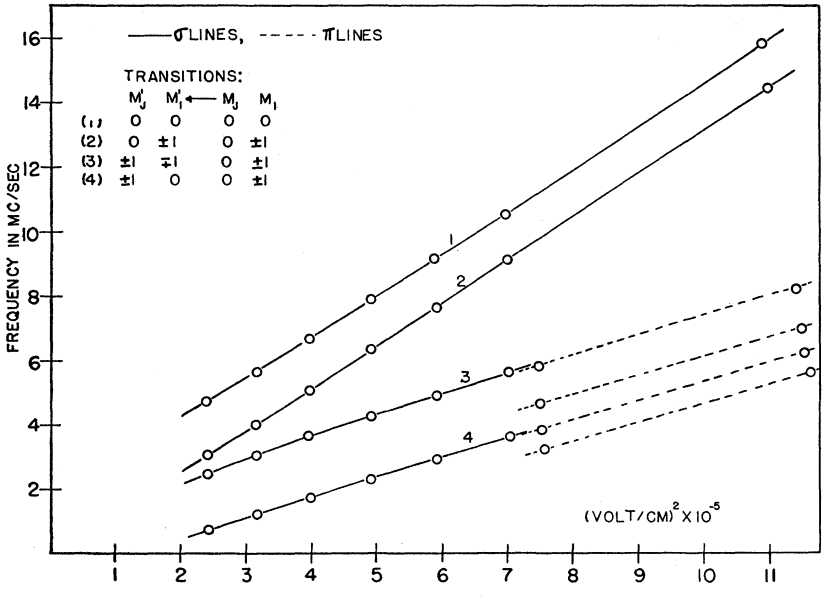

FIG. 3. Graph showing the frequency dependence as function of field strength for the σ and π Stark components of the $J=1 \leftarrow 0$ transition of HCN.

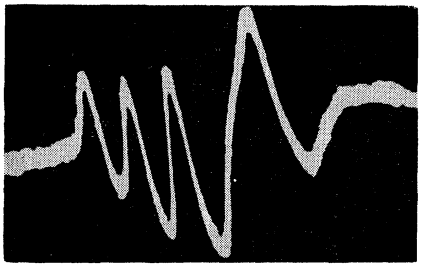

FIG. 4. Oscillogram of the π Stark components of the $J=1 \leftarrow 0$ transition of HCN for the strong field case.

special case $J=1$, $M_J=0$, $M_I=\pm 1$

$$\begin{pmatrix} -\beta+2\alpha-W & -3\alpha+C \\ -3\alpha+C & -2\beta+2\alpha-W \end{pmatrix}=0,$$

where $\beta=\mu^2E^2/20B_0h$ and $\alpha=eQq/20$. The roots are:

$$W=(\beta/2)+2\alpha\pm[(9/4)\beta^2+9\alpha^2+C^2-6\alpha C]^{\frac{1}{2}}$$

$$=\frac{\mu^2E^2}{40B_0h}+\frac{eQq}{10}\pm\left[\frac{9}{4}\left(\frac{\mu^2E^2}{20B_0h}\right)^2+9\left(\frac{eQq}{20}\right)^2+C^2-6\left(\frac{eQq}{20}\right)C\right]^{\frac{1}{2}}.$$

With the displacement of the $J=0$ level, $-\mu^2E^2/6Bh$, this gives the displaced frequency ν to be

$$\nu=\nu_0+\frac{1}{10}eQq+\frac{23}{60}\frac{\mu^2E^2}{\nu_0}\pm\left[\frac{9}{4}\left(\frac{\mu^2E^2}{10\nu_0}\right)^2+9\left(\frac{eQq}{20}\right)^2+C^2-6\left(\frac{eQq}{20}\right)C\right]^{\frac{1}{2}},$$

where ν_0 is the corresponding zero field frequency $2B_0h$. It will be noticed that there is some deviation in the dipole moment calculated for different fields. The frequency shift at these small fields is relatively small, and the dipole moment is rather sensitive to small errors in measurement.

The frequency shifts of one of the π components of the lines of HCN for various field values are given in Table III. Some of the observations were taken on a type P amplifier. To correct for the distortion created by the P amplifier it was necessary to take readings with both the P amplifier and the broad-band amplifier. A small frequency correction had to be introduced to account for the line distortion.

The difficulties in treating HCN by the conventional strong field uncoupling methods are apparent from the changing splitting pattern. Only in the case of the π component corresponding to ±1, $\pm1 \leftarrow 0$, ±1 are the levels nondegenerate and the dipole moments calculable without difficulty. The results of the dipole moment calculations from this transition are given in Table II. It is seen that the moment values are highly consistent within the limits of field variation.

TABLE II. Numerical results from measurements on a σ component.

Transition M_J' $M_I' \rightarrow$ M_J, M_I		
0 ±1	0 ±1	
Field in volts/cm	$\nu-\nu_0$ in Mc/sec	μ in Debye units
490.18	3.031	2.983
561.16	4.000	2.985
629.87	5.079	2.985
700.39	6.348	2.990
768.37	7.687	2.990
836.53	9.143	2.987
1046.20	14.464	2.985
	Averaged value	2.986±0.004

TABLE III. Numerical results from measurements on a π component.

Transition M_J', $M_I' \leftarrow M_J$, M_I		
±1 ±1	0 ±1	
Field in volts/cm	$\nu-\nu_0$ in Mc/sec	μ in Debye units
866.57	4.697	2.979
1282.77	10.012	2.982
1487.02	13.380	2.983
1683.88	17.092	2.984
1897.54	21.643	2.984
2111.02	26.681	2.982
2325.00	32.301	2.981
2532.05	38.305	2.983
2741.29	44.842	2.982
2743.05	44.650[a]	2.982[a]
2948.40	51.657[a]	2.984[a]
	Average value	2.982+0.003

[a] Measured with type P amplifier.

TABLE IV. Averaged results by least squares method of fitting data on three π components.

Transition M_J', $M_I' \leftarrow M_J$, M_I				Equation (ν in Mc/sec, E in volts/cm)	Dipole moment (in Debye units)
∓1	0	0	0	$\nu=\nu_0-0.5169+5.9466\times10^{-6}E^2$	2.985
±1	±1	0	±1	$\nu=\nu_0+0.247+5.9341\times10^{-6}E^2$	2.982
±1	∓1	0	±1	$\nu=\nu_0+1.583+5.9439\times10^{-6}E^2$	2.984
					2.984

Table IV summarizes the results obtained by a least-square evaluation of the data such as that shown in Table III for that of the π components which were carefully measured over a range of fields corresponding to that indicated in Table III. Again the results are consistent with expectation and yield an averaged value of 2.984±0.002 for the moment.

The frequency measurements are accurate to better than 0.005 Mc/sec. The electric field has been measured to an accuracy of a tenth of a percent. Thus an estimate of the absolute error of 0.004 in the values of dipole

moments quoted in Table I may be regarded as conservative. The error in the relative values of the dipole moment is believed to be less. It will be noted that the dipole moment from observation of the line, 2.986 Debye units, is in good agreement with the dipole moment from the π lines, 2.984 Debye units. We choose as the most probable μ the one obtained by averaging values from the four measured components. The final value,

$$\mu = 2.986 \pm 0.004,$$

is in agreement with the less accurate one obtained by Ghosh, Trambarulo, and Gordy,[1] 3.00 ± 0.02 Debye units. Interestingly it is 0.028 Debye greater than the value, 2.957 ± 0.025 Debye units, obtained by Schulman and Townes[2] for the excited bending vibrational state. A difference of this order might be expected in the moments for the ground and vibrational states.

High Stark precision measurements have earlier been made on OCS in the centimeter wave region.[7,13] This "calibrated" OCS molecule provides a convenient reference standard for measuring electric fields or other dipole moments with centimeter-wave spectroscopy. However, this standard, or others that could be similarly established by centimeter wave measurements, is not satisfactory for the millimeter or submillimeter wave region because of the rapidly decreasing sensitivity of the Stark splitting with increasing J. HCN which has a large dipole moment as well as low J transitions originating in the shorter millimeter wave region provides a convenient millimeter wave measuring standard which can be projected into the submillimeter region. Already our measurements on HCN have been privately communicated to C. A. Burrus who has used them for secondary measurements on several other simple molecules in the 1- to 3-mm wave region.[14]

[13] R. G. Shulman and C. H. Townes, Phys. Rev. **77**, 500 (1950).
[14] C. A. Burrus, J. Chem. Phys. **28**, 427 (1958).

PHYSICAL REVIEW VOLUME 119, NUMBER 1 JULY 1, 1960

Born Cross Sections for Inelastic Scattering of Electrons by Hydrogen Atoms. I. $3s$, $3p$, $3d$ States*†

GERARD C. MCCOYD, S. N. MILFORD, AND JOHN J. WAHL
St. John's University, Jamaica, New York

(Received January 20, 1960)

Born cross sections of all $n=3$ to $n=4$ transitions are calculated at ten incident electron energy values in the range 0.67–1400 ev, and those of strong optically allowed $n=3$ to $n=5$ transitions are calculated at five incident electron energy values in the range 1–10 000 ev. The cross sections obtained are much larger than for comparable transitions from the ground state, and the cross sections for transitions which are optically allowed and in which n and l change in the same sense are larger than those for other transitions. For all strong optically allowed transitions the Bethe (dipole) approximations to the Born cross sections are calculated and comparison shows that the Bethe formula gives a good fit to the Born approximation down to relatively low energies (≈ 10 ev).

INTRODUCTION

MOST calculations of atomic cross sections have involved the ground states of atoms. Since very high temperature gases have recently been produced in the laboratory, and since there is now extensive astrophysical investigation of departures from local thermodynamic equilibrium in such gases, there is a need for inelastic collision cross sections for excited states of atoms.

The cross sections for collisions of electrons with excited hydrogen atoms are not only the easiest among all possible atoms to calculate, but also have immediate application to theories of the solar chromosphere.[1] Apart from cross sections for the ground state,[2] the only other previous calculations involve transitions from the $2s$ state[3] and the $2p$ state[4] calculated in the first Born approximation; Goldstein[5] and Yavorsky[6] wrote down general series expressions for the transition $n \rightarrow n'$, but these do not appear to be useful for numerical calculation of the cross sections.

The present paper discusses transitions from the $3s$, $3p$, and $3d$ levels of hydrogen to the $n=4$ and $n=5$

* This work was supported in part by the Office of Naval Research and in part by the Air Force Office of Scientific Research.

† Based in part on a thesis submitted by John J. Wahl to the Graduate School of St. John's University, in partial fulfillment of the requirements for the degree of Master of Science.

[1] See the series of papers by R. N. Thomas and collaborators in the *Astrophysical Journal*, and the forthcoming monograph by R. G. Athay and R. N. Thomas, *Physics of the Solar Chromosphere* (Interscience Publishers, Inc., New York, to be published).

[2] R. McCarroll, Proc. Phys. Soc. (London) **A70**, 460 (1957), summarizes Born calculations; for a summary of more extensive calculations see H. S. W. Massey, *Handbuch der Physik*, edited by S. Flügge (Springer-Verlag, Berlin, 1956), Vol. 36, p. 354.

[3] T. J. M. Boyd, Proc. Phys. Soc. (London) **72**, 523 (1958).

[4] H. S. W. Massey and E. H. S. Burhop, *Electronic and Ionic Impact Phenomena* (Oxford University Press, New York, 1952), p. 170.

[5] L. Goldstein, Ann. phys. **19**, 305 (1933).

[6] B. M. Yavorsky, Compt. rend. acad. sci. U.R.S.S. **43**, 151 (1944).

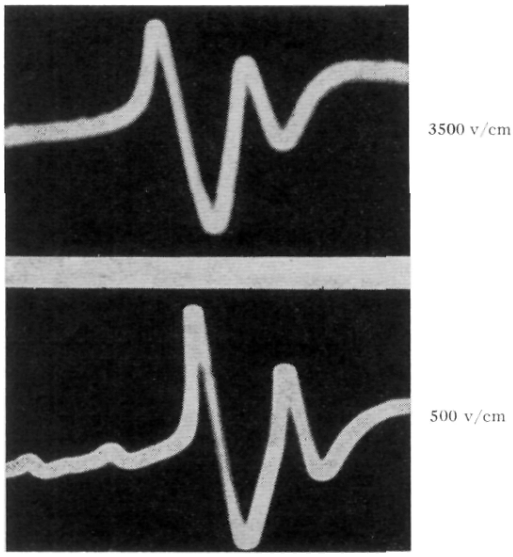

FIG. 2. Cathode ray oscillograms of the σ components for the intermediate (lower) and strong (upper) field splitting of the $J=1 \leftarrow 0$ transition of HCN.

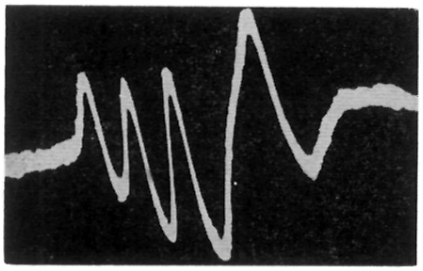

FIG. 4. Oscillogram of the π Stark components of the $J=1 \leftarrow 0$ transition of HCN for the strong field case.